Thermal fluctuations and bending rigidities of graphane and fluorographene at different temperatures

Junjie Chen [a, b, *]

[a] Department of Mechanical and Aerospace Engineering, College of Engineering, University of California, Davis, California, 95616, United States

[b] Department of Energy and Power Engineering, School of Mechanical and Power Engineering, Henan Polytechnic University, Jiaozuo, Henan, 454000, P.R. China

* Corresponding author, E-mail address: junjiem@tom.com

Abstract

Little research has been conducted to determine the thermal properties and phenomena of graphane and fluorographene. A clear understanding of the thermal problems involved is needed, which may provide a basis for further research on other material properties. In the present study, molecular dynamics simulations were performed to investigate the thermal properties of graphane and fluorographene and especially the phenomena involved, including thermal fluctuations and bending rigidities. Furthermore, comparisons of thermal properties and the phenomena involved were made computationally between pristine and functionalised graphene. The thermal fluctuations and bending rigidities were determined at different temperatures. The present study aims to provide a clear understanding of the thermal problems involved in hydrogenated and fluorinated graphene. The results indicated that while thermally excited ripples spontaneously appear in graphene, fully hydrogenated or fluorinated graphene is substantially unrippled due to their very high bending rigidities. There is no significant effect of thermal rippling throughout graphane and fluorographene due to their very high bending rigidities. However, partially hydrogenated or fluorinated graphene exhibits strong thermal fluctuations. Graphene behaves differently from graphane and fluorographene with regard to the dependence of bending rigidity on temperature. Furthermore, significant out-of-plane fluctuations may occur in partially fluorinated graphene. Thermal fluctuations of graphene are more sensitive to temperature than those of graphane and fluorographene.

Keywords: Thermal rippling; Thermal fluctuations; Bending rigidities; Molecular dynamics; Thermal properties; Thermal phenomena

1. Introduction

The basic electronic structure of graphene and, as a consequence, its electric properties are very peculiar [1, 2]. By applying a gate voltage or using chemical doping by adsorbed atoms and molecules, one can create either electron or hole conductivity in graphene that is similar to the conductivity created in semiconductors [3, 4]. However, in most semiconductors there are certain energy levels where electrons and holes do not have allowed quantum states, and, because electrons and holes cannot occupy these levels, for certain gate voltages and types of chemical doping, the semiconductor acts as an insulator. Graphene, on the other hand, does not have an insulator state, and conductivity remains finite at any doping, including zero doping [5, 6]. Existence of this minimal conductivity for the undoped case is a striking difference between graphene and conventional semiconductors [7, 8]. Electron and hole states in graphene relevant for charge-carrier transport are similar to the states of ultra-relativistic quantum particles.

The honeycomb lattice of graphene actually consists of two sublattices, designated A and B, such

that each atom in sublattice A is surrounded by three atoms of sublattice B and vice versa. This simple geometrical arrangement leads to the appearance that the electrons and holes in graphene have an unusual degree of internal freedom, usually called pseudospin [9, 10]. In fact, making the analogy more complete, pseudospin mimics the spin, or internal angular momentum, of subatomic particles. Within this analogy, electrons and holes in graphene play the same role as particles and antiparticles in quantum electrodynamics [11, 12]. At the same time, however, the velocity of the electrons and holes is less than the speed of light. This makes graphene a test bed for high-energy physics: some quantum relativistic effects that are hardly reachable in experiments with subatomic particles using particle accelerators have clear analogy in the physics of electrons and holes in graphene, which can be measured and studied more easily because of their lower velocity [13, 14]. An example is the Klein paradox, in which ultra-relativistic quantum particles, contrary to intuition, penetrate easily through very high and broad energy barriers [15, 16]. Thus, graphene provides a bridge between materials science and some areas of fundamental physics, such as relativistic quantum mechanics.

There is another reason why graphene is of special interest to fundamental science: it is the first and simplest example of a two-dimensional crystal. This means that a solid material that contains just a single layer of atoms arranged in an ordered pattern [17, 18]. Two-dimensional systems are of huge interest not only for physics but also for chemistry. In many respects, two-dimensional systems are fundamentally different from three-dimensional systems [19, 20]. In particular, due to very strong thermal fluctuations of atomic positions that remain correlated at large distances, long-range crystalline order cannot exist in two dimensions. Instead, only short-range order exists, and it does so only on some finite scale of characteristic length, a caveat that should be noted when graphene is called a two-dimensional crystal [21, 22]. For this reason, two-dimensional systems are inherently flexural, manifesting strong bending fluctuations, so that they cannot be flat and are always rippled or corrugated [23, 24]. Graphene, because of its relative simplicity, can be considered as a model system for studying two-dimensional physics and chemistry in general [25, 26]. Other two-dimensional crystals besides graphene can be derived by exfoliation from other multilayer crystals or by chemical modification of graphene, for example, graphane, hydrogenated graphene, and fluorinated graphene [27, 28]. Modern electronics are basically two-dimensional in that they use mainly the surface of semiconducting materials. Therefore, graphene and other two-dimensional materials are considered very promising for many such applications.

In spite of significant efforts to investigate the structural and electronic properties of hydrogenated and fluorinated graphene [29, 30], little research has been conducted to determine their other thermal properties and phenomena, for example, thermal rippling. A clear understanding of the thermal problems involved is needed, which may provide a basis for further research on other material properties [31, 32]. In the present study, molecular dynamics simulations were performed to investigate the thermal properties of graphane and fluorographene and especially the phenomena involved, including thermal fluctuations and bending rigidities at different temperatures. Furthermore, comparisons of thermal properties and the phenomena involved were made computationally between pristine and functionalised graphene. The present study aims to provide a clear understanding of the thermal problems involved in hydrogenated and fluorinated graphene. Particular emphasis is placed upon the thermal rippling of pristine and functionalised graphene at different temperatures.

2. Molecular dynamics modelling

Molecular dynamics simulation may calculate a characteristic and a structure of a system by simulating a motion of an atom in a system constituted by the atom using a computer and may be an important simulation method for evaluating and predicting a structure and characteristic of a substance from a microscopic aspect of the substance. In an actual calculation process, to obtain ideal data, it may

need to expand the scale of the simulation calculation and extend the simulation time, and thus, the simulation calculation may consume considerable time. A temporal step of molecular dynamics simulation may be a few femtoseconds, whereas a computer simulation with millions of steps may correspond to a few femtoseconds in an actual process and the computational amount may be significantly large to reflect an actual macroscopic operation.

Distinguishable conformations exist, and the chair configuration is the most stable structure because of its lowest formation energy. A conformation is any one of the infinite numbers of possible spatial arrangements of atoms in a molecule that result from rotation of its constituent groups of atoms about single bonds. Different conformations are possible for any molecule in which a single covalent bond connects two polyatomic groups, in each of which at least one atom does not lie along the axis of the single bond in question. In general, every distinguishable conformation of a molecule represents a state of different potential energy because of the operation of attractive or repulsive forces that vary with the distances between different parts of the structure. The crystal structure of graphane or fluorographene with armchair edges is illustrated schematically in Figure 1 in a chair conformation. In the present study, molecular dynamics simulations are performed to investigate the thermal properties of the two-dimensional materials and especially the phenomena involved, and their molecules are existed in a chair conformation, in which all the carbon-hydrogen or carbon-fluorine bonds are disposed in a staggered arrangement. The carbon atoms of graphene, graphane, or fluorographene are arranged in a flat, planar structure that is a single atom thick. The hydrogen or fluorine atoms are alternately adsorbed above and below the graphene sheet.

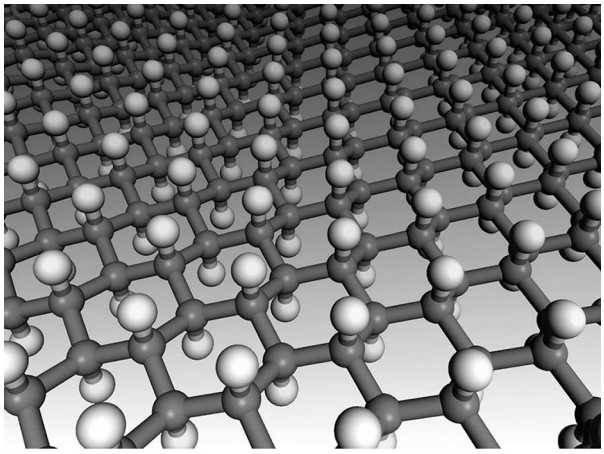

Figure 1. Schematic representation of the crystal structure of graphane or fluorographene with armchair edges in a chair conformation. Grey spheres represent carbon atoms and white spheres represent hydrogen or fluorine atoms.

For the two-dimensional crystals considered here, the total number of carbon atoms are identical to each other. For example, the total number of atoms in graphene is 44,800, and the two-dimensional crystal is 34.0 nm in length and in width. For example, the total number of atoms in graphane is 89,600, and the two-dimensional crystal is 37.0 nm in length and 36.6 nm in width. In some cases, periodic boundary conditions are used in both crystallographic directions. Calculations are performed to resolve the problem by a classical molecular-dynamics code LAMMPS. A Nosé-Hoover thermostat is applied to equilibrate the system throughout the simulation process. For example, thermostats are applied to the two-dimensional crystals to achieve room temperature. Thermostats are then lifted, and the crystals are allowed to freely evolve as "active atoms". The temperatures of the crystals deviate from the initial value during the relaxation process. Consequently, thermostats are reapplied and then lifted periodically until the desired temperature is achieved. The thermal properties of the two-dimensional materials are predicted in the canonical ensemble with a time step of 0.2 femtoseconds. The system is equilibrated for 5 picoseconds and then the equilibrium length is averaged over time, for example, 2 picoseconds at

the specified temperature. The system is modelled by preventing the motion of the terminal atoms on the transverse edge of the crystal structure in the thickness direction to describe the thermal contraction or expansion of the crystalline solid. The progress is realized by fixing two rows of atoms on opposite longitudinal sides in practice, but the motion of the atoms is allowed in the length and width directions to relax the system with a thermal contraction or expansion property.

The amorphous varieties of carbon are based upon microcrystalline forms of graphite [33, 34]. The individual layers of carbon in graphite are called graphene, which has been successfully isolated in single-layer form [35, 36]. The field of graphene science and technology is relatively new [37, 38]. Progress depends not only on the basic science but also on the development of new ways to produce graphene on an industrial scale [39, 40]. Methods proposed include the formation of graphene layers by burning silicon carbide or by chemical vapour deposition of carbon on the surface of some metals such as copper or nickel [41, 42]. These methods will allow the production of samples of graphene that were macroscopically large in two dimensions but still atomically thin [43, 44]. A single-walled carbon nanotube can be described as a long tube formed by wrapping a single graphene sheet into a cylinder, the ends of which are capped by fullerene cages. The fullerene structures, with alternating structures of five hexagons adjacent to one pentagon, form the surface with desired curvature to enclose the volume [45, 46]. The sidewalls of carbon nanotubes are made of graphene sheets consisting of neighbouring hexagonal cells [47, 48]. The thermal properties of the two-dimensional materials and especially the phenomena involved are investigated at temperatures up to 1600 K in order to determine the contraction-expansion transition temperature and the significant difference in specific heat capacity between graphane and fluorographene. The problem of determining the thermodynamic properties at very low temperatures is beyond the ability of the second-generation reactive empirical bond order potential, for example, due to quantum zero energy. In this context, the *ab initio* approach is extremely effective, for example, the density functional theory. In the *ab initio* approach, the calculation proceeds from first principles and makes no use of imported information. The *ab initio* approach is intrinsically reliable because there can be no certainty that a quantity determined in one context is appropriate to a particular molecule. The density functional theory makes it possible to apply the complicated mathematics of quantum mechanics to the description and analysis of the chemical bonding between atoms. The density functional theory can greatly simplify the computations needed to understand the electron bonding between atoms within molecules. The field of graphene science and technology is relatively new, and it remains difficult to determine which applications will prove to be the most popular. Knowledge of the thermal properties and the phenomena involved over a wide range of temperatures may be crucially important to the success in applications in an extreme environment.

The Fourier transform of the out-of-plane atomic displacement is required to determine the height-height correlation function. In particular, the height of each lattice site needs to be defined so that the magnitude of height fluctuations can be determined for the two-dimensional materials. However, the atomic positions are discontinuous and therefore smooth operation is necessary. The problem relates to numerical calculations involving derivatives and different operators on the hexagonal lattice. Consequently, the following procedure is carried out. The present study is focused mainly upon long-wavelength ripple effects. Accordingly, the height of a lattice site can be calculated on the basis of the atomic positions of carbon as follows:

$$h_i = \frac{1}{2}\left(z_i + \frac{1}{3}\left(z_{i,a} + z_{i,b} + z_{i,c} \right) \right), \tag{1}$$

in which h_i is the height of a lattice site, i denotes a carbon atom, z denotes a coordinate variable, and a, b, and c denote three nearest neighbours of atom i. The lattice-site height is used to determine the Fourier components of the out-of-plane atomic displacement using the wave vectors defined by

periodic boundary conditions of the undistorted lattice.

Fundamentally, there are two different approaches to the heat capacity problem. This problem can be solved by numerically calculating the partial derivative of the total energy with respect to the temperature. Specifically, a piecewise-polynomial function of temperature can be defined for the material property with the help of nonlinear curve fitting schemes, which is essential for formulating the physical relationship between the total energy and the temperature. MATLAB and Simulink are used to fit curves to the energy data interactively or programmatically. Kelvin is used as the temperature unit. The heat capacity varies nonlinearly with temperature, and up to four ranges of temperatures are defined. A second-degree polynomial is fitted to the data. Higher-order polynomials may cause oscillations, which will lead to a poorer fit to the data. Finally, the heat capacities can be calculated with the use of finite difference approximations.

A different approach can be adopted to the heat capacity problem. The phonon dispersion relations with the density of states can serve as an approach to this problem, as described below. The heat capacity of the system is stored by its lattice vibrations or phonons and its free conduction electrons

$$C = C_{ph} + C_{el}\,, \tag{2}$$

in which C_{ph} is the contribution from phonons, and C_{el} is the contribution due to electrons. In the present study, the contribution due to electrons is negligible and phonons dominate the heat capacity at all practical temperatures. Consequently, the heat capacity of the system can be calculated by integrating over the phonon density of states with a convolution factor that reflects the energy and occupation of each phonon state

$$c_v(T) = k_B \sum_p \int d(\omega) D_p(\omega) \left(\left(\frac{\hbar\omega}{k_B T} \right)^2 e^{\frac{\hbar\omega}{k_B T}} \left(e^{\frac{\hbar\omega}{k_B T}} - 1 \right)^{-2} \right), \tag{3}$$

wherein k_B is Boltzmann's constant, also referred to as the Boltzmann constant, p is the polarization, $\hbar$ is the reduced Planck's constant, ω is the angular frequency, and D is the phonon density of states. The heat capacity described by the above mathematical formula is evaluated separately for each phonon mode. At nonzero temperatures, the convolution factor is unity if the frequency is zero. The convolution factor decreases smoothly to a value of about 0.1, if $\hbar\omega$ is equal to $6k_BT$. As a consequence, the heat capacity of the material rises with temperature, since more phonon states are occupied. The convolution factor is appreciable, for example, greater than 0.1, if $\hbar\omega$ is less than $6k_BT$. In contrast, if $\hbar\omega$ is greater than $6k_BT$, this factor dampens out the contribution of the phonon density of states to the integral of the heat capacity function. The heat capacity, at least at moderate temperatures, cannot be calculated analytically, as the phonon density of states is in general a complicated function of frequency. Planck's constant is a fundamental physical constant characteristic of the mathematical formulations of quantum mechanics, which describes the behaviour of particles and waves on the atomic scale. Polarization is a property of certain electromagnetic radiations in which the direction and magnitude of the vibrating electric field are related in a specified way. In circular polarization, the electric vector rotates about the direction of propagation as the wave progresses.

The classical or high-temperature limit for the heat capacity expression does not depend upon any specific structure of the system, as formulated by the empirical law of Dulong and Petit. More specifically, the heat capacity is nearly constant at very high temperatures, approaching the in-plane Debye temperature. At sufficiently low temperatures, the contribution from the lowest-frequency optical branch is negligible. In this regime, the density of states is dominated by acoustic phonon modes, and therefore the heat capacity is entirely determined by the acoustic branches. More specifically, the contribution due to optical phonons is negligible if the system is subject to certain

temperature conditions

$$T < T_o \approx \frac{\hbar \omega_o}{6k_B}, \tag{4}$$

where ω_o is the frequency of the lowest-energy optical phonon. In such a situation, the heat capacity of the system can be calculated using the acoustic-phonon dispersion relations. At low temperatures, the heat capacity is typically a power function in which the temperature base is raised to an exponent greater than unity. The precise exponent depends upon the dimensionality of the system and the detailed phonon dispersion relations.

The first Brillouin zone that represents the central cell of the reciprocal lattice is illustrated schematically in Figure 2 for the two-dimensional materials. A Brillouin zone is defined as a Wigner-Seitz primitive cell in the reciprocal lattice. The concept of Brillouin zone is particularly important in the consideration of the electronic structure of solids. The first Brillouin zone represents the central cell of the reciprocal lattice. It contains all points nearest to the enclosed reciprocal lattice point. The boundaries of the first Brillouin zone are determined by planes which are perpendicular to the reciprocal lattice vectors pointing from the centre of the cell to the lattice points nearest to the origin of the cell at their midpoints. Due to the translational invariance of the lattice the wave functions and the energy bands are periodic in the reciprocal space and it is sufficient to consider only the first Brillouin zone for band structure calculations. For example, the diamond structure is invariant not only under translations, but also under several other symmetry operations such as reflections, rotations, or inversion. These symmetry operations are usually denoted as point operations, since they leave at least one point of the lattice invariant, which is not the case for translations. The set of all point operations for a particular crystal structure forms a group which is denoted as point group. The point group of the diamond structure has 48 symmetry elements which are reflected in the symmetry of the first Brillouin zone. The point symmetries of the crystal structure are mirrored in the crystal potential, and hence in the one-particle Hamiltonian used for band structure calculations.

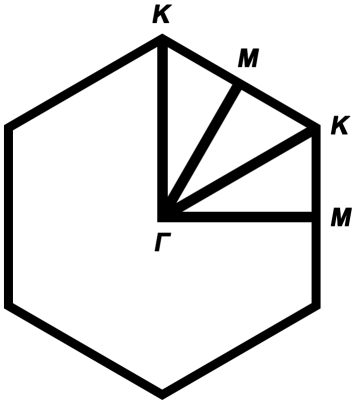

Figure 2. Schematic representation of the first Brillouin zone that represents the central cell of the reciprocal lattice for the two-dimensional materials.

Elemental carbon exists in several forms, each of which has its own physical characteristics [49, 50]. Two of its well-defined forms, diamond and graphite, are crystalline in structure, but they differ in physical properties because the arrangements of the atoms in their structures are dissimilar [51, 52]. A third form, called fullerene, consists of a variety of molecules composed entirely of carbon [53, 54]. Spheroidal, closed-cage fullerenes are called buckyballs, and cylindrical fullerenes are called nanotubes [55, 56]. Yet another form, called amorphous carbon, has no crystalline structure. The phonon dispersion relations along *Γ-M* direction of the first Brillouin zone are described in Figure 3 for graphene with the acoustic and optical modes indicated. The phonon dispersion relations along *Γ-M-K-Γ* direction of the first Brillouin zone are described in Figure 4 for graphane in a chair

conformation. The phonon dispersion relations along *Γ*-*M*-*K*-*Γ* direction of the first Brillouin zone are described in Figure 5 for fluorographene in a chair conformation. The phonon dispersion relations are determined for the two-dimensional materials using Troullier-Martins pseudopotentials and a plane-wave basis set. First-principles calculations are carried out at an energy cutoff of roughly 40 Hartree. The Brillouin zone is sampled using a Monkhorst-Pack k-point mesh of 30 × 30 × 1 for the electronic structure. The structures are fully relaxed so that the magnitude of all forces is less than 5 × 10^{-5} Hartree per Bohr and the magnitude of all stresses is less than 5 × 10^{-7} Hartree per cubic Bohr. The dynamical properties are determined by applying density-functional perturbation theory, which allows for calculations of any phonon frequency without requiring use of a supercell. There exist substantial differences in phonon spectrum between the two-dimensional materials. For instance, the low-frequency, medium-frequency, and high-frequency groups of phonon branches for graphane are clearly separated from each other. In contrast, the frequency groups for fluorographene are indistinguishable from each other. In particular, graphene is a two-dimensional system with three acoustic branches and three optic branches. At low wave vectors near the centre of the first Brillouin zone, two acoustic modes have very high sound velocities and linear dispersions, namely a longitudinal mode, with a group velocity of about 21.3 kilometres per second, and an in-plane transverse mode, with a group velocity of about 13.6 kilometres per second. Additionally, the third out-of-plane transverse mode can be described by an approximately quadratic dispersion relation, where the frequency is equal to δq^2, with δ being a value of about 6.2 × 10^{-7} square metres per second. Accordingly, the heat capacity of the two-dimensional material from the in-plane modes should yield dependence upon the temperature squared, since the phonon density of states is proportional to the frequency. Additionally, the heat capacity from the out-of-plane mode should be linear in temperature, as the phonon density of states is constant. For an isolated graphene sheet, the behaviour of heat capacity should be linear in temperature at very low temperatures when the quadratic out-of-plane acoustic modes dominate, followed by a transition to behaviour of temperature squared approximately due to the linear longitudinal and transverse acoustic modes and eventually by "flattening" to a constant as the high Debye temperature is approached, in the classical limit.

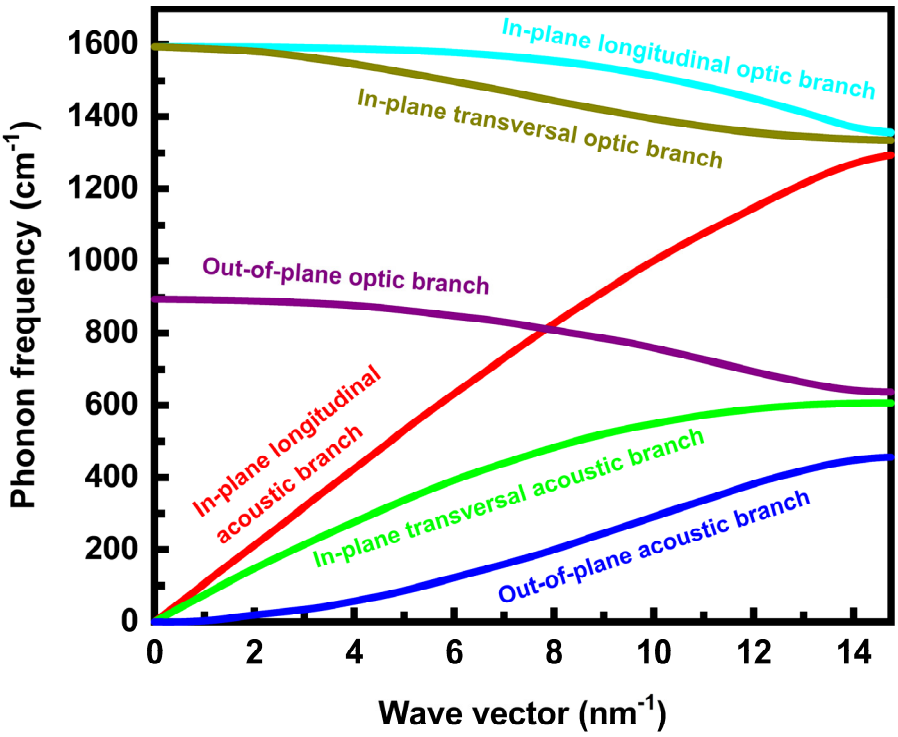

Figure 3. Phonon dispersion relations along *Γ*-*M* direction of the first Brillouin zone for graphene with the acoustic and optical modes indicated.

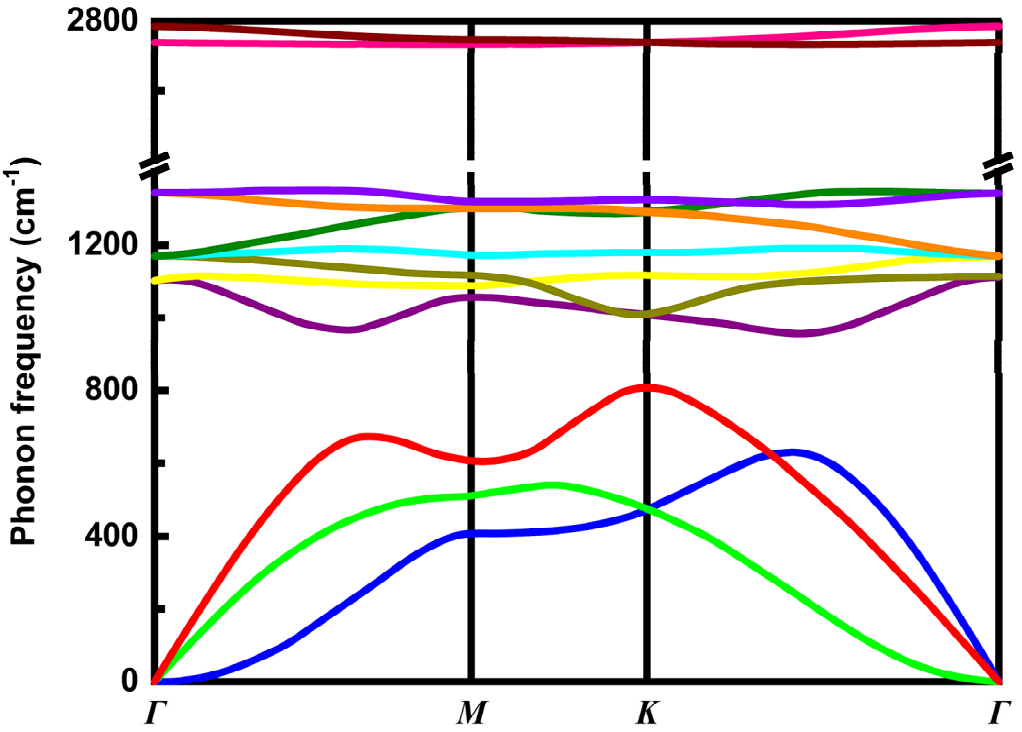

Figure 4. Phonon dispersion relations along *Γ-M-K-Γ* direction of the first Brillouin zone for graphane in a chair conformation.

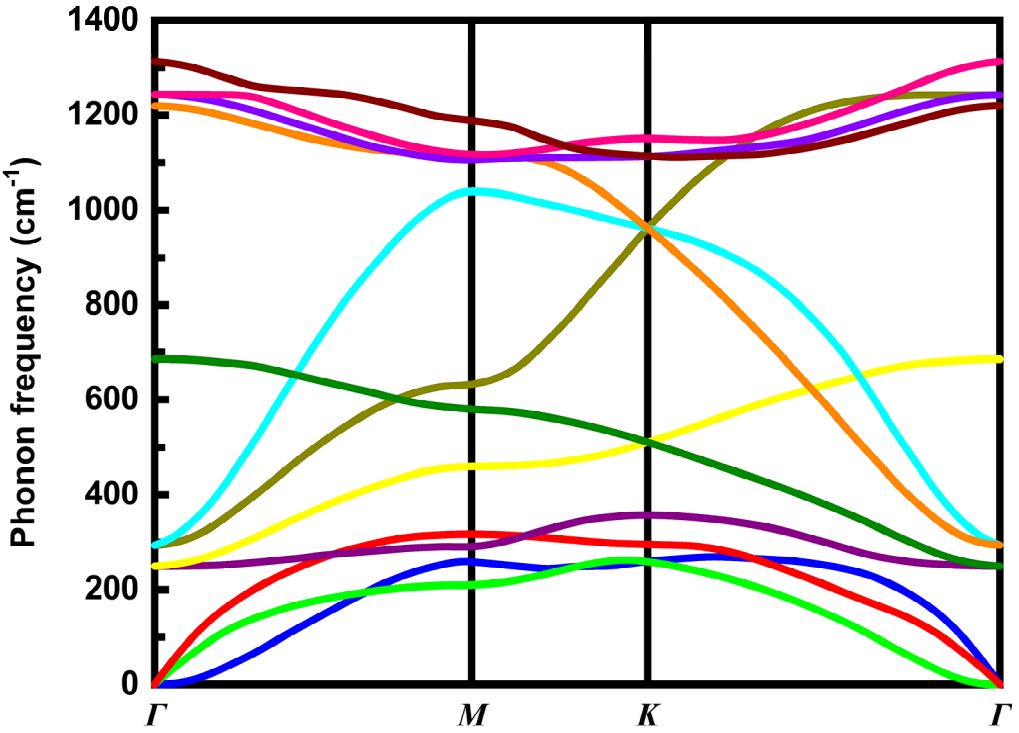

Figure 5. Phonon dispersion relations along *Γ-M-K-Γ* direction of the first Brillouin zone for fluorographene in a chair conformation.

3. Results and discussion

Hydrogenation is a chemical reaction between molecular hydrogen and an element or compound, ordinarily in the presence of a catalyst. The reaction may be one in which hydrogen simply adds to a double or triple bond connecting two atoms in the structure of the molecule or one in which the addition of hydrogen results in dissociation of the molecule. Typical hydrogenation reactions include the reaction of hydrogen and nitrogen to form ammonia and the reaction of hydrogen and carbon

monoxide to form methanol or hydrocarbons, depending on the choice of catalyst. The catalysts most commonly used for hydrogenation reactions are the metals nickel, platinum, and palladium and their oxides. Fluorinated compositions are known to possess many outstanding properties. The range of these properties is indicated by the broad range of utilities for fluorinated compositions. It is debatable whether or not hydrogenation or fluorination enhances the tendency for buckling and rippling. Out-of-plane thermal fluctuations may occur in these two-dimensional materials. However, how large the thermal fluctuations need to be determined.

The effect of temperature on the mean square height fluctuation is illustrated in Figure 6 for graphene, graphane, and fluorographene. Out-of-plane thermal fluctuations may occur in the two-dimensional materials. A right-Y scale is added to the graph and the graphane and fluorographene's data are plotted against this scale, as indicated by the rightwards arrows. A phonon is a unit of vibrational energy that arises from oscillating atoms within a crystal. Any solid crystal consists of atoms bound into a specific repeating three-dimensional spatial pattern called a lattice. Because the atoms behave as if they are connected by tiny springs, their own thermal energy or outside forces make the lattice vibrate. This generates mechanical waves that carry heat and sound through the material. A packet of these waves can travel throughout the crystal with a definite energy and momentum. As the temperature increases from 50 K to 800 K, the mean square height fluctuation is increased from about 80 nm^2 to about 200 nm^2 for graphene. For graphane and fluorographene, however, the mean square height fluctuation does not vary significantly with temperature, for example, in the range from about 6 nm^2 to about 12 nm^2. Therefore, graphane and fluorographene do not develop significant corrugation or long-wavelength ripples. The temperature affects the mean square height fluctuation of graphene more remarkably than that of graphane and fluorographene.

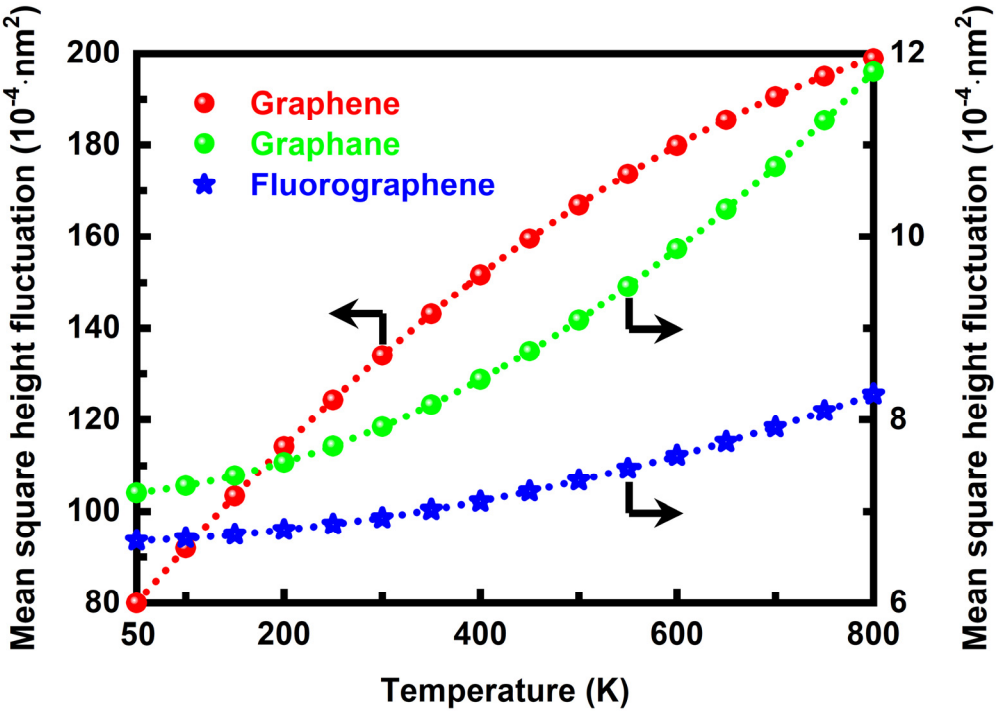

Figure 6. Effect of temperature on the mean square height fluctuation of graphene, graphane, and fluorographene. Out-of-plane thermal fluctuations may occur in the materials. A right-Y scale is added to the graph and the graphane and fluorographene's data are plotted against this scale, as indicated by the rightwards arrows.

A material property is an intensive property of a material. A physical property or chemical property does not depend on the amount of the material. These quantitative properties may be used as a metric by which the benefits of one material versus another can be compared, thereby aiding in

materials selection. A material property may also be a function of one or more independent variables, for example, temperature. Materials properties often vary to some degree according to the direction in the material in which they are measured, a condition referred to as anisotropy. Materials properties that relate to different physical phenomena often behave linearly in a given operating range. Modelling them as linear functions can significantly simplify the differential constitutive equations that are used to describe the property. Equations describing relevant materials properties are often used to predict the attributes of a system. The thermodynamic properties of materials are intensive thermodynamic parameters which are specific to a given material. The thermal properties of partially hydrogenated or fluorinated graphene have attracted much attention [57, 58]. It is necessary to investigate the thermal rippling phenomena of the two-dimensional materials in certain situations.

The effect of hydrogenation or fluorination degree on the mean square height fluctuation of graphene at room temperature is illustrated in Figure 7 in which the results obtained for fully hydrogenated or fluorinated graphene are also presented. The degree of hydrogenation or fluorination can greatly affect the mean square height fluctuation of graphene. As the hydrogenation or fluorination degree increases, the mean square height fluctuation of graphene first increases and then decreases. Fluorination causes the maximum fluctuation magnitude to become more pronounced. Specifically, partially fluorinated graphene is about four times the maximum mean-square height fluctuation of partially hydrogenated graphene. More specifically, the maximum mean-square height fluctuation is about 0.179 nm^2 for partially fluorinated graphene and about 0.048 nm^2 for partially hydrogenated graphene. In some cases, partially fluorinated graphene is more than five times the mean-square height fluctuation of partially hydrogenated graphene. However, hydrogenation or fluorination does not enable the maximum mean-square height fluctuation if graphene is half-hydrogenated or half-fluorinated. The maximum mean-square height fluctuation will be achieved if the degree of hydrogenation or fluorination is about 60 percent. The mean-square height fluctuation tends to become zero if graphene is fully hydrogenated or fluorinated.

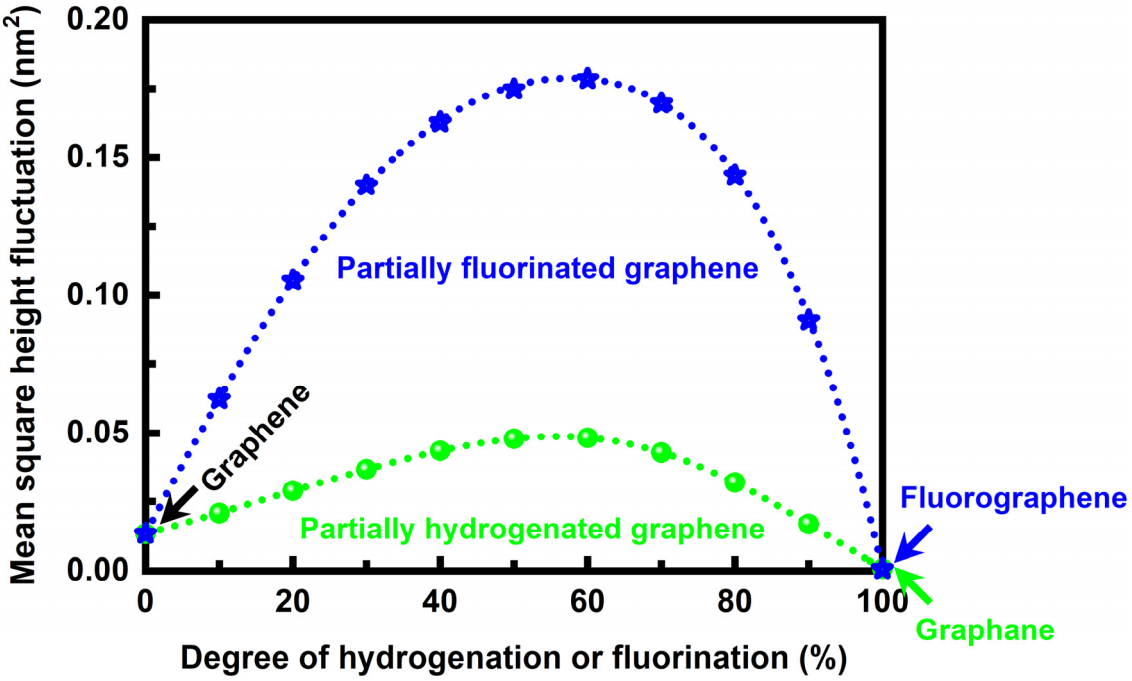

Figure 7. Effect of hydrogenation or fluorination degree on the mean square height fluctuation of graphene at room temperature. The mean square height fluctuations of fully hydrogenated or fluorinated graphene are also indicated.

Graphene provides a bridge between materials science and some areas of fundamental physics. The effect of temperature on the bending rigidity is investigated for graphene, graphane, and

fluorographene. The bending rigidity is defined as the force couple required to bend a fixed non-rigid structure by one unit of curvature, or as the resistance offered by a structure while undergoing bending. The bending rigidity of the two-dimensional material is determined by the Young's modulus, Poisson's ratio, and cube of the elastic thickness of the material. Young's modulus describes the elastic properties of a solid undergoing tension or compression in only one direction. Sometimes referred to as the modulus of elasticity, Young's modulus is equal to the longitudinal stress divided by the strain. Young's modulus is meaningful only in the range in which the stress is proportional to the strain. Poisson's ratio is the ratio of lateral strain to the longitudinal strain.

The effect of temperature on the bending rigidity is illustrated in Figure 8 for graphene, graphane, and fluorographene. For hydrogenated or fluorinated graphene, the amplitudes of intrinsic ripples may be reinforced due to the effect of random thermal fluctuations of hydrogen and fluorine atoms. Accordingly, the ripple amplitudes may rise and fall rapidly, although the intrinsic ripples of hydrogenated or fluorinated graphene are of different amplitude. However, significant corrugation or long-wavelength ripples will not be developed if the material is rigid. Specifically, the bending rigidity of fully hydrogenated or fluorinated graphene is significantly higher than that of graphene, and therefore there are no significant corrugation or long-wavelength ripple effects throughout graphane and fluorographene. Interestingly, the temperature affects the bending rigidity of either graphane or fluorographene more remarkably than that of graphene. Consequently, the bending rigidity of graphane or fluorographene is sensitive to temperature. Additionally, the bending rigidity of graphane or fluorographene has negative dependence upon temperature, while the bending rigidity of graphene has positive dependence upon temperature. Graphene behaves anomalously with temperature in this respect. As the temperature increases from 50 K to 800 K, the bending rigidity is increased from about 1.06 eV to about 1.32 eV for graphene, and it is decreased from about 9.76 eV to about 5.58 eV for graphane and from about 6.27 eV to about 5.06 eV for fluorographene, respectively.

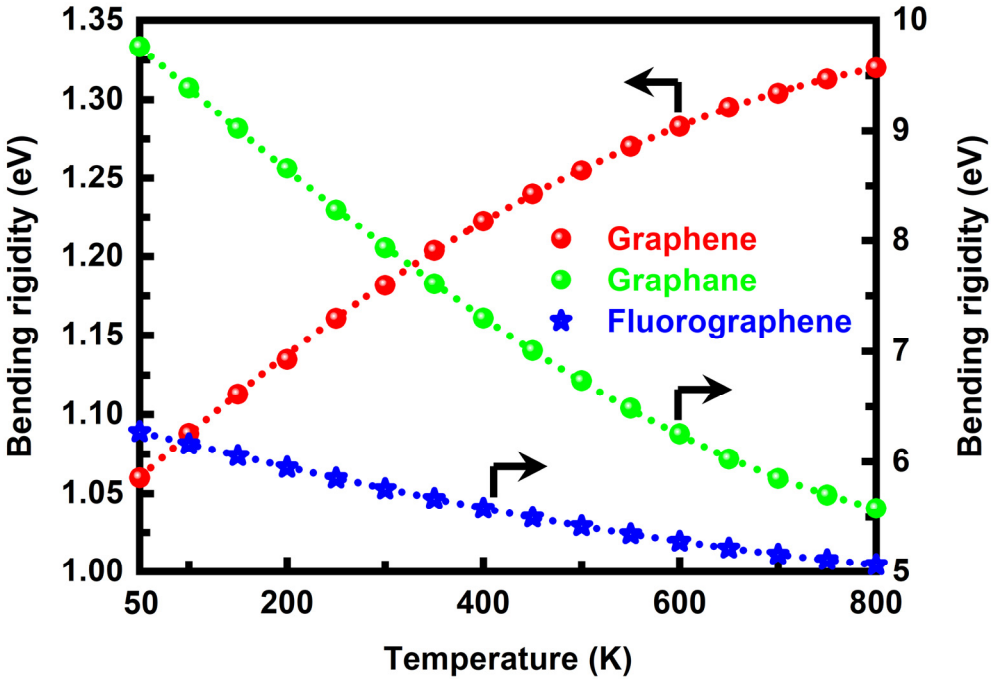

Figure 8. Bending rigidity of graphene, graphane, and fluorographene at different temperatures. Significant corrugation or long-wavelength ripples will not be developed if the material is rigid. A right-Y scale is added to the graph and the graphane and fluorographene's data are plotted against this scale, as indicated by the rightwards arrows.

For graphene, the dependence of bending rigidity upon temperature is highly debated in the literature [59, 60]. Both negative and positive dependences are determined theoretically, in the range

from about 0.85 eV to about 10 eV [61, 62], which is consistent with that predicted here. It is very difficult to measure the bending rigidity because of the contribution from extrinsic stiffening from in-plane strain or out-of-plane corrugations [59, 60]. However, a recent experimental study has demonstrated that the bending rigidity of bilayer graphene increases sightly with temperature [60], as presented here for graphene. Over a temperature range from 280 K to 400 K, the bending rigidity of bilayer graphene, as measured by experiments, varies from about 3.0 eV to about 3.6 eV [60]. Additionally, the bending rigidity of bilayer graphene may be twice that of graphene [63]. Accordingly, an estimated bending rigidity in the range from about 1.5 eV to about 1.8 eV can be obtained for graphene in the temperature range indicated above. As the temperature increases from 280 K to 400 K, the bending rigidity predicted in the present study by the model increases from about 1.17 eV to about 1.22 eV. Another experimental study has demonstrated that the bending rigidity of graphene is about 1.30 eV over a temperature range from 110 K to 500 K [64]. Consequently, the predictions are substantially in agreement with the measurements.

There is a need to investigate the other thermal properties of graphane and fluorographene and especially the phenomena involved in the thermodynamic and transport processes, for example, enthalpy and entropy, under various conditions of temperature and pressure. Enthalpy and entropy are extensive properties [65, 66] and thus the magnitudes of these state functions depend upon the amount of material in the thermodynamic system. More specifically, it is neither necessary nor convenient to determine the absolute values of enthalpy or entropy of graphane and fluorographene [65, 66]. Consequently, intensive studies will be carried out to solve the problem related to the thermal properties and phenomena of the materials and their interrelations.

4. Conclusions

Molecular dynamics was used to investigate the thermal properties of graphane and fluorographene and especially the phenomena involved in the thermodynamic process when subjected to changes in temperature, including thermal expansion coefficients, heat capacities, thermal fluctuations, and bending rigidities, which have profound implications for the development of thermal technology at the nanoscale. Additionally, first-principles calculations were carried out to determine the structural configurations of the two-dimensional materials. Furthermore, comparisons of thermal properties and the phenomena involved were made between pristine and functionalised graphene. The main conclusions are summarised as follows:

- While graphene tends to spontaneous bending and ripple formation, fully hydrogenated or fluorinated graphene is substantially unrippled.
- There is no significant effect of thermal rippling throughout graphane and fluorographene due to their very high bending rigidities.
- Graphene behaves differently from graphane and fluorographene with regard to the dependence of bending rigidity on temperature.
- Thermally excited ripples spontaneously appear in partially hydrogenated or fluorinated graphene due to strong out-of-plane fluctuations.
- Significant thermal fluctuations may occur in partially fluorinated graphene.
- The temperature affects the thermal fluctuations of graphene more remarkably than those of graphane and fluorographene.

References

[1] I. Calizo, S. Ghosh, W. Bao, F. Miao, C.N. Lau, and A.A. Balandin. Raman nanometrology of graphene: Temperature and substrate effects. *Solid State Communications*, Volume 149, Issues

27-28, 2009, Pages 1132-1135.
[2] J. Fernández-Rossier, J. J. Palacios, and L. Brey. Electronic structure of gated graphene and graphene ribbons. *Physical Review B*, Volume 75, Issue 20, 2007, Article Number: 205441.
[3] N.M.R. Peres. The electronic properties of graphene and its bilayer. *Vacuum*, Volume 83, Issue 10, 2009, Pages 1248-1252.
[4] T.O. Wehling, M.I. Katsnelson, and A.I. Lichtenstein. Adsorbates on graphene: Impurity states and electron scattering. *Chemical Physics Letters*, Volume 476, Issues 4-6, 2009, Pages 125-134.
[5] K. Nomura and A.H. MacDonald. Quantum hall ferromagnetism in graphene. *Physical Review Letters*, Volume 96, Issue 25, 2006, Article Number: 256602.
[6] S. Adam, E.H. Hwang, E. Rossi, and S.D. Sarma. Theory of charged impurity scattering in two-dimensional graphene. *Solid State Communications*, Volume 149, Issues 27-28, 2009, Pages 1072-1079.
[7] D.W. Horsell, A.K. Savchenko, F.V. Tikhonenko, K. Kechedzhi, I.V. Lerner, and V.I. Fal'ko. Mesoscopic conductance fluctuations in graphene. *Solid State Communications*, Volume 149, Issues 27-28, 2009, Pages 1041-1045.
[8] A.C. Ferrari, J.C. Meyer, V. Scardaci, C. Casiraghi, M. Lazzeri, F. Mauri, S. Piscanec, D. Jiang, K.S. Novoselov, S. Roth, and A.K. Geim. Raman spectrum of graphene and graphene layers. *Physical Review Letters*, Volume 97, Issue 18, 2006, Article Number: 187401.
[9] R. Danneau, F. Wu, M.F. Craciun, S. Russo, M.Y. Tomi, J. Salmilehto, A.F. Morpurgo, and P.J. Hakonen. Shot noise measurements in graphene. *Solid State Communications*, Volume 149, Issues 27-28, 2009, Pages 1050-1055.
[10] J.P. Robinson, H. Schomerus, L. Oroszlány, and V.I. Fal'ko. Adsorbate-limited conductivity of graphene. *Physical Review Letters*, Volume 101, Issue 19, 2008, Article Number: 196803.
[11] L. Vitali, C. Riedl, R. Ohmann, I. Brihuega, U. Starke, and K. Kern. Spatial modulation of the Dirac gap in epitaxial graphene. *Surface Science*, Volume 602, Issue 22, 2008, Pages L127-L130.
[12] V.N. Popov, L. Henrard, and P. Lambin. Resonant Raman spectra of graphene with point defects. *Carbon*, Volume 47, Issue 10, 2009, Pages 2448-2455.
[13] Z. Papić, M.O. Goerbig, and N. Regnault. Theoretical expectations for a fractional quantum Hall effect in graphene. *Solid State Communications*, Volume 149, Issues 27-28, 2009, Pages 1056-1060.
[14] A.H.C. Neto, F. Guinea, N.M.R. Peres, K.S. Novoselov, and A.K. Geim. The electronic properties of graphene. *Reviews of Modern Physics*, Volume 81, Issue 1, 2009, Pages 109-162.
[15] A.H.C. Neto, V.N. Kotov, J. Nilsson, V.M. Pereira, N.M.R. Peres, and B. Uchoa. Adatoms in graphene. *Solid State Communications*, Volume 149, Issues 27-28, 2009, Pages 1094-1100.
[16] K. Ziegler. Random-gap model for graphene and graphene bilayers. *Physical Review Letters*, Volume 102, Issue 12, 2009, Article Number: 126802.
[17] S. Adam and S.D. Sarma. Transport in suspended graphene. *Solid State Communications*, Volume 146, Issues 9-10, 2008, Pages 356-360.
[18] A.J.M. Giesbers, U. Zeitler, S. Neubeck, F. Freitag, K.S. Novoselov, and J.C. Maan. Nanolithography and manipulation of graphene using an atomic force microscope. *Solid State Communications*, Volume 147, Issues 9-10, 2008, Pages 366-369.
[19] R. Jackiw and S.-Y. Pi. Chiral gauge theory for graphene. *Physical Review Letters*, Volume 98, Issue 26, 2007, Article Number: 266402.
[20] G. Borghi, M. Polini, R. Asgari, and A.H. MacDonald. Fermi velocity enhancement in monolayer and bilayer graphene. *Solid State Communications*, Volume 149, Issues 27-28, 2009, Pages 1117-1122.
[21] W.A. de Heer, C. Berger, X. Wu, P.N. First, E.H. Conrad, X. Li, T. Li, M. Sprinkle, J. Hass, M.L.

Sadowski, M. Potemski, and G. Martinez. Epitaxial graphene. *Solid State Communications*, Volume 143, Issues 1-2, 2007, Pages 92-100.
[22] P. Kleinert. Anomalous ac electric field effect in bilayer graphene. *Physica B: Condensed Matter*, Volume 404, Issue 21, 2009, Pages 4015-4017.
[23] R. Bistritzer and A.H. MacDonald. Electronic cooling in graphene. *Physical Review Letters*, Volume 102, Issue 20, 2009, Article Number: 206410.
[24] M. Koshino and T. Ando. Diamagnetic response of graphene multilayers. *Physica E: Low-dimensional Systems and Nanostructures*, Volume 40, Issue 5, 2008, Pages 1014-1016.
[25] M. Koshino and T. Ando. Electronic structures and optical absorption of multilayer graphenes. *Solid State Communications*, Volume 149, Issues 27-28, 2009, Pages 1123-1127.
[26] D. Pandey, R. Reifenberger, and R. Piner. Scanning probe microscopy study of exfoliated oxidized graphene sheets. *Surface Science*, Volume 602, Issue 9, 2008, Pages 1607-1613.
[27] P.G. Silvestrov and K.B. Efetov. Quantum dots in graphene. *Physical Review Letters*, Volume 98, Issue 1, 2007, Article Number: 016802.
[28] I. Calizo, S. Ghosh, W. Bao, F. Miao, C.N. Lau, and A.A. Balandin. Raman nanometrology of graphene: Temperature and substrate effects. *Solid State Communications*, Volume 149, Issues 27-28, 2009, Pages 1132-1135.
[29] A. Bostwick, J. McChesney, T. Ohta, E. Rotenberg, T. Seyller, and K. Horn. Experimental studies of the electronic structure of graphene. *Progress in Surface Science*, Volume 84, Issues 11-12, 2009, Pages 380-413.
[30] I. Martin, Y.M. Blanter, and A.F. Morpurgo. Topological confinement in bilayer graphene. *Physical Review Letters*, Volume 100, Issue 3, 2008, Article Number: 036804.
[31] L.M. Malard, D.L. Mafra, S.K. Doorn, and M.A. Pimenta. Resonance Raman scattering in graphene: Probing phonons and electrons. *Solid State Communications*, Volume 149, Issues 27-28, 2009, Pages 1136-1139.
[32] J. Nilsson, A.H.C. Neto, F. Guinea, and N.M.R. Peres. Electronic properties of graphene multilayers. *Physical Review Letters*, Volume 97, Issue 26, 2006, Article Number: 266801.
[33] T. Enoki and K. Takai. The edge state of nanographene and the magnetism of the edge-state spins. *Solid State Communications*, Volume 149, Issues 27-28, 2009, Pages 1144-1150.
[34] L.M. Malard, M.A. Pimenta, G. Dresselhaus, and M.S. Dresselhaus. Raman spectroscopy in graphene. *Physics Reports*, Volume 473, Issues 5-6, 2009, Pages 51-87.
[35] A. Luican, G. Li, and E.Y. Andrei. Scanning tunneling microscopy and spectroscopy of graphene layers on graphite. *Solid State Communications*, Volume 149, Issues 27-28, 2009, Pages 1151-1156.
[36] F.V. Tikhonenko, D.W. Horsell, R.V. Gorbachev, and A.K. Savchenko. Weak localization in graphene flakes. *Physical Review Letters*, Volume 100, Issue 5, 2008, Article Number: 056802.
[37] D.W. Boukhvalov. Tuneable molecular doping of corrugated graphene. *Surface Science*, Volume 604, Issues 23-24, 2010, Pages 2190-2193.
[38] M. Taghioskoui. Trends in graphene research. *Materials Today*, Volume 12, Issue 10, 2009, Pages 34-37.
[39] J. Yan, Y. Zhang, S. Goler, P. Kim, and A. Pinczuk. Raman scattering and tunable electron-phonon coupling in single layer graphene. *Solid State Communications*, Volume 143, Issues 1-2, 2007, Pages 39-43.
[40] D. Graf, F. Molitor, K. Ensslin, C. Stampfer, A. Jungen, C. Hierold, and L. Wirtz. Raman imaging of graphene. *Solid State Communications*, Volume 143, Issues 1-2, 2007, Pages 44-46.
[41] B.A. Bernevig, T.L. Hughes, and S.-C. Zhang. The quantum Hall effect in graphene from a lattice perspective. *Solid State Communications*, Volume 143, Issues 1-2, 2007, Pages 20-26.

[42] I.L. Aleiner and K.B. Efetov. Effect of disorder on transport in graphene. *Physical Review Letters*, Volume 97, Issue 23, 2006, Article Number: 236801.
[43] K. Yang. Spontaneous symmetry breaking and quantum Hall effect in graphene. *Solid State Communications*, Volume 143, Issues 1-2, 2007, Pages 27-32.
[44] J.E. Drut and T.A. Lähde. Is graphene in vacuum an insulator? *Physical Review Letters*, Volume 102, Issue 2, 2009, Article Number: 026802.
[45] Z. Jiang, Y. Zhang, Y.-W. Tan, H.L. Stormer, and P. Kim. Quantum Hall effect in graphene. *Solid State Communications*, Volume 143, Issues 1-2, 2007, Pages 14-19.
[46] A.C. Ferrari. Raman spectroscopy of graphene and graphite: Disorder, electron-phonon coupling, doping and nonadiabatic effects. *Solid State Communications*, Volume 143, Issues 1-2, 2007, Pages 47-57.
[47] J.-W. Rhim and K. Moon. Spin stiffness of graphene and zigzag graphene nanoribbons. *Physical Review B*, Volume 80, Issue 15, 2009, Article Number: 155441.
[48] M. Polini, R. Asgari, Y. Barlas, T. Pereg-Barnea, and A.H. MacDonald. Graphene: A pseudochiral Fermi liquid. *Solid State Communications*, Volume 143, Issues 1-2, 2007, Pages 58-62.
[49] H.B. Heersche, P. Jarillo-Herrero, J.B. Oostinga, L.M.K. Vandersypen, and A.F. Morpurgo. Induced superconductivity in graphene. *Solid State Communications*, Volume 143, Issues 1-2, 2007, Pages 72-76.
[50] D.A. Abanin, P.A. Lee, and L.S. Levitov. Charge and spin transport at the quantum Hall edge of graphene. *Solid State Communications*, Volume 143, Issues 1-2, 2007, Pages 77-85.
[51] Z. Liu, K. Suenaga, P.J.F. Harris, and S. Iijima. Open and closed edges of graphene layers. *Physical Review Letters*, Volume 102, Issue 1, 2009, Article Number: 015501.
[52] Y.-W. Son, M.L. Cohen, and S.G. Louie. Energy gaps in graphene nanoribbons. *Physical Review Letters*, Volume 97, Issue 21, 2006, Article Number: 216803.
[53] E. McCann, D.S.L. Abergel, and V.I. Fal'ko. Electrons in bilayer graphene. *Solid State Communications*, Volume 143, Issues 1-2, 2007, Pages 110-115.
[54] F. Guinea, A.H.C. Neto, and N.M.R. Peres. Electronic properties of stacks of graphene layers. *Solid State Communications*, Volume 143, Issues 1-2, 2007, Pages 116-122.
[55] M.L. Sadowski, G. Martinez, M. Potemski, C. Berger, and W.A. de Heer. Magnetospectroscopy of epitaxial few-layer graphene. *Solid State Communications*, Volume 143, Issues 1-2, 2007, Pages 123-125.
[56] Q. Wang. Simulations of the bending rigidity of graphene. *Physics Letters A*, Volume 374, Issue 9, 2010, Pages 1180-1183.
[57] M. Pashangpour. Electronic transport properties of partially hydrogenated and fluorinated borophene, a DFT study. *Computational Materials Science*, Volume 168, 2019, Pages 74-80.
[58] Y. Pedram, F. Marsusi, and S. Yousefbeigi. Melting process of fluorinated graphene: A molecular dynamics study. *Chemical Physics Letters*, Volume 780, 2021, Article Number: 138920.
[59] K. Ziegler. Robust transport properties in graphene. *Physical Review Letters*, Volume 97, Issue 26, 2006, Article Number: 266802.
[60] S.D. Eder, S.K. Hellner, S. Forti, J.M. Nordbotten, J.R. Manson, C. Coletti, and B. Holst. Temperature-dependent bending rigidity of *AB*-stacked bilayer graphene. *Physical Review Letters*, Volume 127, Issue 26, 2021, Article Number: 266102.
[61] J. Nam, J. Yang, Y. Zhao, and K.S. Kim. Chemical vapor deposition of graphene and its characterizations and applications. *Current Applied Physics*, Volume 61, 2024, Pages 55-70.
[62] S. Santra, A. Bose, K. Mitra, and A. Adalder. Exploring two decades of graphene: The jack of all trades. *Applied Materials Today*, Volume 36, 2024, Article Number: 102066.
[63] K.V. Zakharchenko, J.H. Los, M.I. Katsnelson, and A. Fasolino. Atomistic simulations of structural

and thermodynamic properties of bilayer graphene. *Physical Review B*, Volume 81, Issue 23, 2010, Article Number: 235439.

[64] A.A. Taleb, H.K. Yu, G. Anemone, D. Farías, and A.M. Wodtke. Helium diffraction and acoustic phonons of graphene grown on copper foil. *Carbon*, Volume 95, 2015, Pages 731-737.

[65] B. Wunderlich and Y. Jin. The thermal properties of four allotropes of carbon. *Thermochimica Acta*, Volume 226, 1993, Pages 169-176.

[66] D.E. Hagen and S.H.S. Salk. Entropy and enthalpy change in hydrated ion clusters. *Chemical Physics*, Volume 102, Issue 3, 1986, Pages 459-466.